FERMILAB-CONF-17-048-TD
(accepted)

Magnetic Quench Antenna for MQXF quadrupoles

M. Marchevsky, G. Sabbi, S. Prestemon, T. Strauss, S. Stoynev and G. Chlachidze

***Abstract*—High-field MQXF-series quadrupoles are presently under development by LARP and CERN for the upcoming LHC luminosity upgrade. Quench training and protection studies on MQXF prototypes require a capability to accurately localize quenches and measure their propagation velocity in the magnet coils. The voltage tap technique commonly used for such purposes is not a convenient option for the 4.2 m-long MQXF-A prototype, nor can it be implemented in the production model. We have developed and tested a modular inductive magnetic antenna for quench localization. The base element of our quench antenna is a round-shaped printed circuit board containing two orthogonal pairs of flat coils integrated with low-noise preamplifiers. The elements are aligned axially and spaced equidistantly in 8-element sections using a supporting rod structure. The sections are installed in the warm bore of the magnet, and can be stacked together to adapt for the magnet length. We discuss the design, operational characteristics and preliminary qualification of the antenna. Axial quench localization capability with an accuracy of better than 2 cm has been validated during training test campaign of the MQXF-S1 quadrupole.**

***Index Terms*—Accelerator magnets, quench, magnetic analysis, magnetic sensors.**

I. Introduction

THE Nb_3Sn 12 T and 150 mm aperture quadrupoles of MQXF series developed by LARP collaboration and CERN are at the core of the planned LHC luminosity upgrade [1]. Three major magnet models are being constructed: MQXF-S with a magnetic length of 1 m, MQXF-A of 4.2 m, and MQXF-B of 7.15 m. The latter two models will be combined in a structural assembly at LHC, having four magnets of "A" type and two of "B" type, while the shorter "S" model is being built and tested to validate and optimize the common design, and ensure it meets the performance requirements [2,3]. Testing campaign of the first MQXF-S has been recently completed by LARP, and will be followed by tests of the MQXF-A prototype. It includes quench training, protection and field quality studies. In the course of these tests, quench locations in the windings have to be determined to verify uniformity of training and consistency with the existing electromagnetic and mechanical stress models. Also, quench propagation velocity is an important parameter that needs to be measured to verify consistency of the quench protection modeling. While traditionally such information is obtained using voltage taps distributed within the coil windings, it is not a particularly suitable method for the MQXF series. Firstly, given the length of MQXF-A and the expected range of quench propagation velocities being similar to that in other Nb_3Sn magnets of similar design [4-6], one would require at least ~20 taps around the pole turn alone of each coil to observe quench propagation between the two neighboring taps within the allowed (typically < 5 ms) quench detection and validation window. Secondly, in the production models the amount of taps is usually minimized to reduce risks of local mechanical electrical breakdown.

In view of these considerations, a magnetic quench antenna is a viable alternative, allowing to localize quenches remotely and non-invasively and to measure their propagation dynamics. Numerous types of quench antennas have been developed in the past for use with various accelerator magnets [7-11]. Our present design is based upon the previously validated concept [12] of quench localization based on detecting gradient of the axial field component in the magnet bore arising from a normal zone formation in the superconducting cable. It incorporates pairs of dipole-bucked pickup coils that are orthogonal to each other in the *xy* plane, and axially aligned along the magnet bore *z*-axis to sense time derivatives of dB_z/dx and dB_z/dy respectively. To achieve easy adaptability to MQXF models of different length and inter-operability with the field quality measurements, our antenna is constructed as a modular structure suitable for installation in the ~130 mm-diameter warm bore ("anti-cryostat") of the magnet aligned with its central axis. In the present work, we present details of conceptual and practical design of the quench antenna, and demonstrate its operational capabilities in the training tests of MQXF-S1quadrupole.

II. Design and Construction

A. Operational principle and sensitivity estimate

Quench development in a superconducting Rutherford cable would normally cause two kinds of transient effects associated with current re-distribution around the hot spot, as sketched in Fig. 1a. The first one is a breakdown of the solenoidal current flow path formed with strand twist around the cable central axis, and a corresponding "leakage" of the stray field from the cable interior [13]. Also, as the initial normal zone is likely to grow non-symmetrically with respect to cable central axis (for example, due to local magnetic field being stronger along the inner cable edge), it will cause a corresponding current flow distortion [14-16]. Both effects result in the appearance of a non-zero axial field component the vicinity of the hot spot that

Manuscript received September 6, 2016.

This work was supported by the US Department of Energy through the US LHC Accelerator Research Program (LARP).

M. Marchevsky, G. Sabbi and S. Prestemon are with Lawrence Berkeley National Laboratory, Berkeley, CA 94720 USA (e-mail: mmartchevskii@lbl.gov).

T. Strauss, S. Stoynev and G. Chlachidze are with the Fermi National Accelerator Laboratory, Batavia, IL 80510 USA

Operated by Fermi Research Alliance, LLC under Contract No. DE-AC02-07CH11359 with the United States Department of Energy.

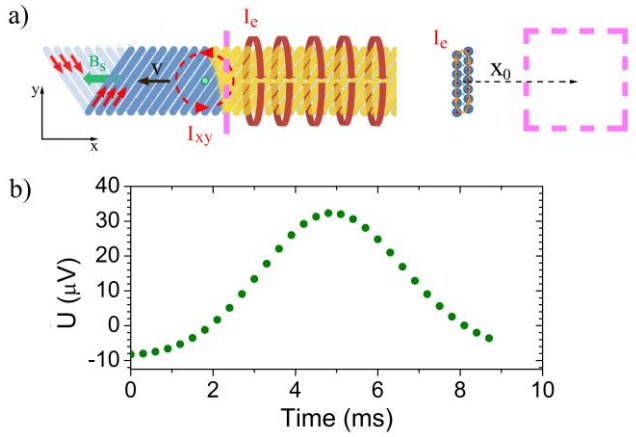

Fig. 1. (a) A sketch showing quench propagation in a Rutherford cable. The normal zone expands to the right causing "leakage" of the solenoidal field form the cable interior, as well as current redistribution near the normal zone boundary. Both effects can be simulated as a set of current loops building up along the cable length. When quench front passes along the antenna pickup coil (shown in dashed line) an inductive signal is generated. (b) The transient inductive voltage calculated for a 25x25 mm-sized rectangular pickup loop placed at x_0=55 mm from the quenching cable.

can be picked up by the sensor coil of the quench antenna. We choose to sense transients of the in-plane gradient of the axial field rather than the field itself, in order to improve accuracy of spatial localization of quench locations and reduce antenna sensitivity to the magnetic noise. A similar approach was taken in [17] where axial field antenna was used to localize quenches in a high-field Nb_3Sn dipole.

To estimate the expected level of antenna voltages due to a quench, we use the simulation approach and software developed and described in [11], and approximate the expanding normal zone as a linear "row" of adjacent circular mini-loops of current occupying the cable cross-section (18.15x1.52 mm) and growing stepwise, row by row in the orthogonal direction along the cable axis thus emulating increasing "leakage" of the stray field from within the expanding normal zone. A single round current loop sized with the cable width, and orthogonal to the mini-loops of the expanding array is placed at the expansion boundary in the cable plane, thus accounting for the effect of planar current re-distribution in the cable. Both assumptions work well provided $R_a << R_s$, where R_a is the inter-strand resistance, and R_s is the strand resistance per cable pitch at hot spot temperature. The latter condition seems to be always true for Nb_3Sn cables at T>~ 150 K. [18]. All loops in our simulation carry the same current I_l given by $I_l=I_{cab}\ (d_{st}/b)$, where d_{st} is the linear step size along the cable axis in our simulation (we have chosen d=3 mm), and b is the cable twist pitch (109 mm). We assume velocity of the normal zone interface of 10 m/s and the net current in the cable I_{cab} = 15 kA (~70% of I_{ss} at 1.9 K). A square probe loop (25x25 mm) placed at a distance (center-to-center) of 55 mm from the cable axis and axially aligned with z-axis is chosen as an equivalent approximation for a single 90-deg sectoral coil of the antenna that would fit into the available space in the inner bore. We ignore the opposite dipole-bucked coil in this simple estimate, since most of the varying flux will be enclosed by the coil nearest to the

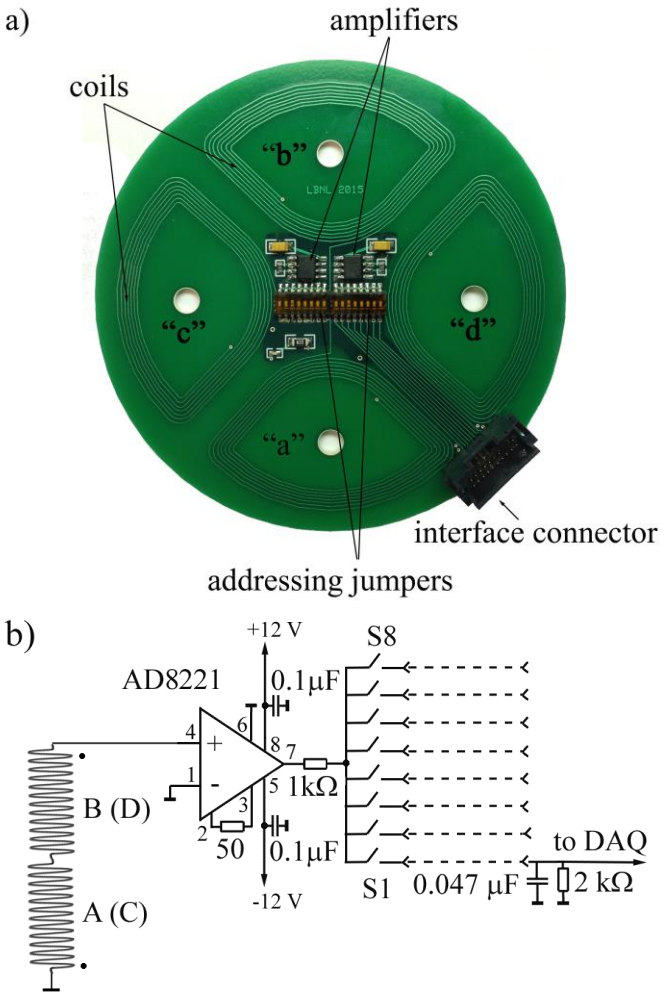

Fig. 2. (a) A photograph of the assembled antenna board (single element). (b) The electrical schematic of a single antenna sub-element (two sub-elements per board). Two oppositely placed quarter-circle flat coils are dipole bucked and their inductive voltage is amplified using low-noise on-board instrumentational amplifier.

quenching cable. Using these parameters, our simulation yields peak inductive voltage in the probe loop of ~$3.2x10^{-5}$ V generated when the quench front passes along the antenna element. For practical purposes, a factor of ~10^4 in signal amplification would be then desirable for matching the antenna output to the input range of a typical data acquisition system. We achieve such gain by having 12-turn coils in each 90-deg antenna element sector in combination with instrumentational amplifiers of gain ~650 installed directly on the antenna boards. Also notable is that the simulated signal persists over ~4 ms which translates into a corresponding 4 cm distance along the z-axis for the given quench propagation velocity, thus providing a rough estimate for the expected axial resolution of the antenna.

B. Practical design

The antenna elements are cut of a 4-layer 0.6 mm-thick printed circuit board, and are 95 mm in diameter. Two identical sub-elements are accommodated at each board. Each sub-element consists of a dipole-bucked pair of sectorial 90-

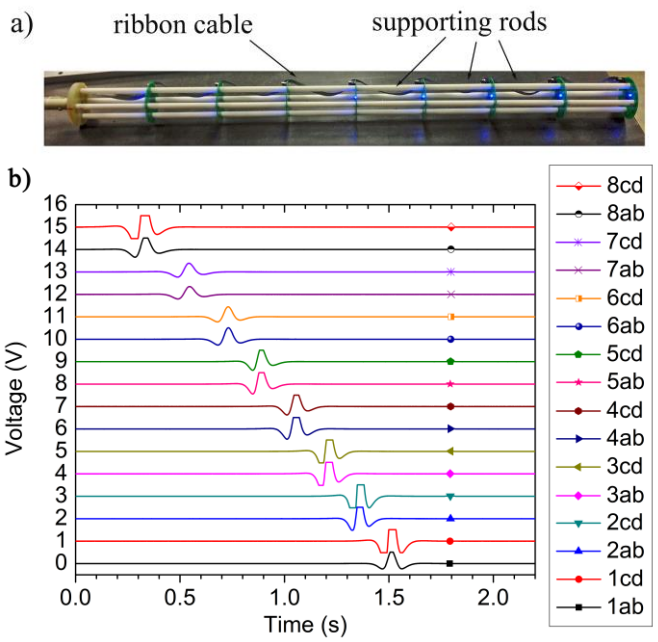

Fig. 3. (a) A photograph of the fully assembled and powered up quench antenna section.(b) Voltages measured at the antenna outputs while a small permanent magnet is moved along the length of the antenna, right to left at ~0.5 m/s velocity. Every two consecutive channels correspond to a single antenna element, with the first element (1ab, 1cd) being the closest to the G10 support baseplate. Traces were progressively offset by 1 V on the vertical axis for clarity.

degree wide flat coils that are mutually rotated by a 180 degree angle (coil pairs are denoted as "ab" and "cd"). Each flat coil contains 12 printed turns (trace width is 0.2 mm) distributed equally between the top and bottom layer of the board. The two inner layers of the board are used for distributing external power to the amplifiers, and, partially, to route some antenna output signals around the interface connector. In the center of the board, two identical preamplifier circuits, one for each sub-channel, are assembled. Also near the board center, there are two blocks of commutation jumpers (8 jumpers per block) allowing to address the preamplifier output to a specific pin of the interface connector. This addressing solution enables use of a flat 20-wire ribbon cable to interface all eight antenna elements of the section, thus carrying 16 independent signals (two per each element), the +12 V and -12 V power lines, and the grounding line. At the side of one jumper block, a miniature LED power-up indicator is installed. A photo of the assembled board is shown in Fig 2a, and the electrical schematic of a single antenna sub-element is shown in Fig. 2b. We use AD8221 low-noise instrumentational amplifiers that were set to gain 1000 using 50 Ω resistor installed between it terminals 2 and 3. In order to prevent parasitic oscillations in the circuit due to inductive and capacitive cross-talk along the long ribbon cable, we added a distributed filter circuit, having 1 kΩ resistor load at the board in series with the RC circuit (0.047 μF and 2 kΩ) terminating each signal line inside the connector box installed at the far end of the ~6 m-long ribbon cable. The filter circuitry effectively reduced the antenna gain to ~650 and narrowed the output bandwidth to ~0-10 kHz. The latter, however, is still sufficient for observing quench propagation based on the simulation data (Fig 1b), while the high-frequency noise is being effectively cut out. In the future the low-pass filter can be adjusted as necessary, to allow for studies of fast transients and flux jump dynamics, up to the full bandwidth of the preamplifier of ~1 MHz. For additional reduction of parasitic electromagnetic noise existing in the magnet test facility, the entire flat ribbon cable was later inserted into a copper-mesh shield, while the coil areas on boards were laminated at one side with a ground-terminated 0.1 mm-thick aluminum foil.

The fully assembled antenna section is shown in Fig 3a. Eight boards are mounted together using plastic rods passing through the board sector centers, and separating the boards by 15.3 cm distance axially, thus yielding the full length of the section of 107.1 cm. The chosen inter-element separation ensures a full length coverage by the antenna of the MQXF-S magnet straight section (100.2 cm), with a small overlap to the coil ends. Also, per our simulation, the element separation should be sufficient to clearly separate quench location axially based on the antenna voltages. For testing the antenna with MQXF-S magnet, the entire section is attached to the supporting round G10 baseplate terminated with an insertion rod for handing the antenna in the warm bore. For the 4.2-m long MQXF-A magnet, four identical antenna sections will be stacked in the warm bore on top of each other, each added section rotated 90 degree clockwise with respect to its lower neighbor in order to accommodate the four ribbon cables coming out of the bore along the sides of the antenna assembly.

A final electrical checkout of the antenna section was conducted prior to its installation in the magnet. It showed a consistently low noise not exceeding 2 mV p-p at all amplifier outputs. A small flexible permanent magnet (of whiteboard type) was moved by hand at a speed of ~0.5/m s along the antenna sides, and antenna voltages were recorded using Yokogawa WE900 simultaneous DAQ sampling continuously at 2 kHz. Consistent time-shifted voltage responses of ~ 1 V in amplitude were measured at all sub-element outputs, as shown in the plot of Fig. 3b.

III. Antenna Validation During Training Study of the MQXF-S1 Quadrupole

We have installed the antenna in the warm bore of MQXF-S1 quadrupole (a first MQXF-S prototype tested at FNAL), and used it to determine quench locations during training studies of this magnet at 1.9 K. The antenna layout overlaying the magnet coil geometry is shown in Fig 4a. Each coil of the magnet was instrumented with 16 voltage taps for quench localization, and the antenna was interfaced to the DAQ of the magnet test facility, sampling at 7.1 kHz (DAQ design speed is 10 kHz) for all signals, including the voltage taps. Only 13 antenna channels (out of 16 available) were interfaced in this test. The data acquisition was set for the time window of 2 s centered at the quench trigger arrival time (denoted as "0 s" in the plots). The trigger was issued when either the total or the imbalance voltage registered by the quench detection system

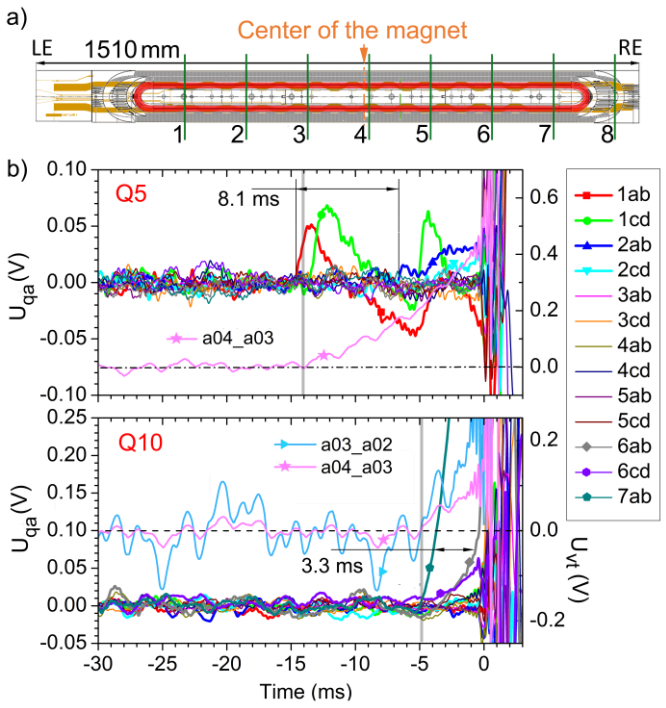

Fig. 4. (a) A sketch showing location of the quench antenna elements on top of the MQXF-S1 coil (inner layer projection shown). The inner multi-turn of the coil is outlined in red. (b) Top plot: quench antenna and voltage tap signals for quench #5 occurring near lead end of the coil in the inner layer inner multi-turn. A delay between the voltage onset time in the neighboring channels "1" and "2" suggest quench propagation velocity of ~ 18.9 m/s. Bottom plot: quench antenna and voltage tap signals for quench #10 occurring near the return end of the coil in the inner layer inner multi-turn. In both quenches a simultaneous rise of voltage across the coil section, and in the quench antenna element was recorded.

increased above its pre-defined threshold setting. In Fig. 4b measurement results for two training quenches are shown: (quench #5) at 17806 A, and another (quench #10) at 18642 A. For analysis purposes all acquired signals were up-sampled at 4 times the original acquisition rate, and then fitted with spline interpolation. Both quenches occurred in the inner layer multi-turn section of the MQXF-S1 coil "3" (marked red in the sketch of Fig. 4a), as evidenced by the rising voltage across the corresponding voltage tap pair a4_a3. While that section of the coil was the only one participating in quench #5, voltage rise was also detected in the neighboring outer multi-turn section monitored by the tap pair a03_a02 in quench #10. In both quenches, Coil "3" of the magnet was facing sector "c" of the quench antenna. One should note, that quenching in multi-turn sections was prevalent in MQXF-S1 training, and the considered two quenches are representative of this magnet behavior. In quench #5 (Fig. 4b, top plot) a voltage above noise level was first detected in "ab" and "cd" channels of the element "1" (closest to the "lead end" of the magnet) at t = -14.0 ms, and within ~0.4 ms of the onset of a voltage rise across the a03_a02 tap pair. In ~8.1 ms following the initial detection a voltage rise was also detected at the element "2" of the antenna. This suggest localization of the quench #5 at the coil lead end, and yields a rough estimate of quench propagation velocity of ~18.9 m/s. Given the ~ ±0.5 ms timing uncertainty in voltage onset between "ab", and "cd" signals, an accuracy of ~2 cm in quench localization can be expected from the antenna. We speculate that the "double peak" feature in voltage traces of the element "1" may be related to quench boundary passing along that element twice at different times. In such scenario, quenching would begin at an axial position in-between the element "1" and the top end of the multi-turn, followed by a simultaneous two-way propagation of the quench boundary towards the coil central region and around its lead end. In quench #10 (Fig. 4b, bottom plot), voltage rise is initially detected at the channel "ab" of the element "7": it is abrupt and simultaneous with the voltage onset across the a4_a3 tap pair. Then ~2 ms later voltage onset is detected at the element "6". However, it rises in a more graduate fashion, taking ~3.3 ms to reach the same positive derivative as that of the channel "ab" of element "7". We believe, this may be related to a quench propagation into the outer multi-turn; in fact, voltage onset at the channel "6" is very close in time to the a2_a3 tap signal rising above its noise level. However, exact determination is difficult, and more analysis is required involving numerical simulations of antenna signals for various possible scenarios of quench propagation. Also, additional simulations will be conducted to enable a full potential of the antenna in distinguishing which side (left or right with respect to the coil central line) is quenching, relying on the polarity and relative voltage amplitude of the channels.

IV. Conclusion

We have designed and constructed a printed circuit board-based axial field quench antenna for localizing quenches in high-field accelerator magnets. The eight element section of the antenna has being qualified during the training study of the MQXF-S1 quadrupole. Adequate sensitivity and ability to localize quenches axially with ~2 cm accuracy has been verified, and an initial estimate of quench propagation velocity along the straight section of the magnet has been done. Quench antenna has proven to be an essential tool in MQXF-S testing campaign, as it enabled axial localization of quenches within the multi-turn coil sections that would be not possible if voltage taps alone were used for quench diagnostics. For future use in the 4.2-m long MQXF-A magnet four identical antenna sections based on the current prototype will be built. Additional benchmarking of the antenna setup against voltage tap-based quench localization, as well as studies of quench propagation, flux jump dynamics and magnetic instabilities will be conducted in the future tests of MQXF prototypes.

Acknowledgment

We are thankful to Tom Lipton, Jason Duval and especially James Swanson for the careful assembly of the antenna parts. Technical and logistic support of the FNAL magnet test facility personnel is gratefully acknowledged.

References

[1] G. G. Apollinari, I. Béjar Alonso, O. Brüning, M. Lamont, and L. Rossi, High-Luminosity Large Hadron Collider (HL-LHC): Preliminary Design Report. Geneva: CERN, 2015. [Online]: http://cds.cern.ch/record/2116337

[2] P. Ferracin, G. Ambrosio, M. Anerella, F. Borgnolutti, R. Bossert, D. Cheng, D. R. Dietderich, H. Felice, A. Ghosh, A. Godeke, S. Izquierdo Bermudez, P. Fessia, S. Krave, M. Juchno, J. C. Perez, L. Oberli,

G. Sabbi, E. Todesco, and M. Yu, “Magnet design of the 150 mm aperture low-quadrupoles for the High Luminosity LHC,” IEEE Trans. Appl. Supercond., vol. 24, no. 3, June 2014, pp.1–6.

[3] G. Ambrosio, “Nb_3Sn high field magnets for the High Luminosity LHC upgrade project,” IEEE Trans. Appl. Supercond., vol. 25, no. 3, June 2015, pp. 1–7.

[4] H. Bajas, G. Ambrosio, M. Anerella, M. Bajko, R. Bossert, L. Bottura., S. Caspi, D. Cheng, A. Chiuchiolo, G. Chlachidze, D. Dietderich, H. Felice, P. Ferracin, J. Feuvrier, A. Ghosh, C. Giloux, A. Godeke, A. R. Hafalia, M. Marchevsky, E. Ravaioli, G. L. Sabbi, T. Salmi, J. Schmalzle, E. Todesco, P. Wanderer, X. Wang, M. Yu, “Test Results of the LARP HQ02b Magnet at 1.9 K”, IEEE Trans. Appl. Supercond. vol. 25, no 3, 2015, Art. ID 4003306.

[5] A. V. Zlobin, N. Andreev, G. Apollinari, B. Auchmann, E. Barzi, S. Izquierdo Bermudez, R. Bossert, M. Buehler, G. Chlachidze, J. DiMarco, M. Karppinen, F. Nobrega, I. Novitski, L. Rossi, D. Smekens, M. Tartaglia, D. Turrioni, G. Velev, “Quench Performance of a 1 m Long Single Aperture 11 T Nb_3Sn Dipole Model for LHC Upgrades”, IEEE Trans. Appl. Supercond. v. 23, no 3, 205, Art. ID 4002209.

[6] M. Calvi, E. Floch, S. Kouzue, A. Siemko, “Improved quench localization and quench propagation velocity measurements in the LHC superconducting dipole magnets”, IEEE Trans. Appl. Supercond. 15, 2005, pp. 1209-1212.

[7] D. Leroy, J. Krzywinski, V. Remondino, L. Walckiers, R. Wolf, “Quench observation in LHC superconducting one meter long dipole models by field perturbation measurements”, IEEE Trans. Appl. Supercond. 3, 1993, pp. 781-784.

[8] T. Ogitsu, A. Devred, K. Kim, J. Krzywinski, P. Radusewicz, R. I. Schermer, T. Kobayashi, K. Tsuchiya, J. Muratore, P. Wanderer, “Quench antenna for superconducting particle accelerator magnets”, IEEE Trans. Magnetics, 30, 1994, pp. 2273-2276.

[9] T. Ogitsu, A. Terashima, K. Tsuchiya, G. Ganetis, J. Muratore, P. Wanderer, “Quench antennas for RHIC quadrupole magnets”, IEEE Trans. Magn. 32, 1996, pp. 1390-1392.

[10] K. Sasaki, T. Ogitsu, N. Obuch, K. Tsuchia, “Study of quench propagation with quench antennas”, Nucl. Instr. Meth. Phys. Res. A 416 1998 pp. 9-17.

[11] M .A. Tartaglia, S. Feher, A. Hocker, M. Lamm, P. Schlabach, C. Sylvester, J. C. Tompkins, “Quench antenna studies of mechanical and quench performance in Fermilab interaction region quadrupoles for LHC”, IEEE Trans. Appl. Supercond., 16, 2006, pp. 441-444.

[12] M. Marchevsky, J. DiMarco, H. Felice, A. R. Hafalia, J. Joseph; J. Lizarazo, X. Wang; G. Sabbi., “Magnetic detection of quenches in high-field accelerator magnets,” IEEE Trans. Appl. Supercond., vol. 23, no. 3, Jun. 2013, Art. ID. 9001005.

[13] S. Takacs, “Current and magnetic field distribution in finite superconucting cables”, Supercond. Sci. Technol. 15, 2002, pp. 377-1384.

[14] A. Verwej, “Electrodynamics of superconducting cables in accelerator magnets“, PhD thesis, University of Twente, 1995.

[15] N. A. Buznikov, A. A. Pukhov, A. L. Rakhmanov and V. S. Vysotsky, “Current redistribution between strands and quench process in a superconducting cable”, Cryogenics 36, 1996, pp. 275-281.

[16] S. Jongeleen, D. Leroy, A. Siemko and R. Wolf, “Quench localization and current redistribution after quench in superconducting dipole magnets wound with Rutherford-type cables”, IEEE Trans. Appl. Supercond. 7, 1997, pp. 179-182.

[17] M. Marchevsky, A. R. Hafalia, D. Cheng, S. Prestemon, G. Sabbi, H. Bajas, and G. Chlachidze, “Axial-Field Magnetic Quench Antenna for the Superconducting Accelerator Magnets”, IEEE Trans. Appl. Supercond., 25, vol. 3, Jun. 2015, Art. ID. pp. 9500605.

[18] T. Salmi, G. Ambrosio, S. Caspi, G. Chlachidze, M. Dhallé, H. Felice, P. Ferracin, M. Marchevsky, G. L. Sabbi, and H. H. J. ten Kate, “Quench protection challenges in long Nb_3Sn accelerator magnets”, AIP Conf. Proc. 1434, 2011, pp. 656-663.